ORIGINAL RESEARCH PAPER

Hydrothermal Synthesis, Structural and Catalytic Studies of $CuBi_2O_4$ Nanoparticles

Fatemeh Soleimani [1], Mahdi Salehi [1]*, Ahmad Gholizadeh [2]

[1] *Department of chemistry, Semnan University, Semnan, Iran*
[2] *School of Physics, Damghan University (DU), Damghan, Iran*

Received: 2017-06-08 Accepted: 2017-08-11 Published: 2017-09-01

ABSTRACT
In the present work $CuBi_2O_4$ nano-spinel has been synthesized via mild hydrothermal method at 180°C for 10 h. The synthesized nanomaterials were characterized by several techniques to emphasis the structure and properties of produced materials. The crystal structure was investigated by X-ray powder diffraction method and the values of the refined unit cell volume and the structure properties were studied by using the Rietveld analysis is done using Fullprof program. The results shew the formation of tetrahedral structure with space group P4/ncc for this sample. Also, the morphologies of the synthesized materials were figured out by field emission scanning electron microscope (FE-SEM). According to the FESEM images, several nano cubic form of particles grew on micro spherical particles. As well, the catalytic performance of obtained $CuBi_2O_4$ was studied in Biginelli reaction. The reaction conditions of this study optimized by experimental design method. This experiment stablished high catalytic performance of copper bismuth oxide in compare with some other metal oxide catalysts. Also, the results shew this product is reusable homogenous catalyst.

Keywords: *$CuBi_2O_4$; Hydrothermal Method; Catalytic activity; Structural study*

How to cite this article

Soleimani F, Salehi M, Gholizadeh A. Hydrothermal Synthesis, Structural and Catalytic Studies of $CuBi_2O_4$ Nanoparticles. J. Nanoanalysis., 2017; 4(3): 239-246. DOI: 10.22034/jna.2017.542053.1019

INTRODUCTION

Catalytic technology has important role on economy growth, therefore, the method of producing, beginning materials of catalyst and the yield of process are undeniable, so that these factors are considered in this research. Synthesizing 3,4 dihydropyrimidin-2-(1H)-ones (DHPMs) as its usage in biology and pharmacology is one of the most important reactions in organic chemistry [1, 2], such as antiviral, anti-inflammatory, antibacterial and antitumor [3, 4]. This three-component reaction, scheme 1, is known as Biginelli reaction [5]. One negative point of view to this reaction is the low yield of the products [6], therefore, many publications try to offer various catalysts for improving the efficiency of the reaction, among them metal oxides are known as heterogeneous catalyst like: $ZnO/MTSA.SiO_2$ [7], TiO_2-MWCNT [8], MnO_2-MWCNT [9], Al_2O_3, CuO [10], RuO_2 [11], Fe_3O_4-MWCNT[12], $Bi_2Mn_2O_7$ [13] and so forth. Copper bismuth oxide is p-type spinel metal oxide which has been synthesized by several methods like: solid state [14], metal organic decomposition[15, 16],

* Corresponding Author Email: msalehi@semnan.ac.ir

electrochemical method [17], sol-gel method [18], sono-chemical approach [19], microwave method [20], thermal deposition [20], hydrothermal synthesis [21], and complexation [22]. The mild hydrothermal method which is used in this work creates spherical morphology for $CuBi_2O_4$ nanoparticles. Some features of $CuBi_2O_4$ lead to using this oxide in different fields. For example, high oxidation protentional causes to use this metal oxide as cathodes in lithium batteries [23]. Also, its narrow band gap energy causes to use as sensitizer semiconductors [15, 24]. Also, The low photon energy leads to using as strong response to visible light [24]. Some other characteristics such as photocatalytic activity [25], dielectric properties [26], magnetic features [27] have been investigated recently. There is no previous research to stablish heterogeneous catalytic activity of $CuBi_2O_4$ so far. Therefore, we try to present structural and catalytic properties of this sample in this investigation by using reasonable data. Preparing pure phase of $Cubi_2O_4$ was denotated by X-ray powder diffraction method and the structure properties were studied by using X'Pert package and Fullprof program. Also, FT-IR and TGA analysis confirmed synthesizing this spinel structure and FE-SEM determined its morphology.

EXPERIMENTAL DETAILS

All chemicals were of analytical grade, obtained from commercial sources (Merck company), and used without further purification. Phase identifications were performed on a powder X-ray diffractometer D5000 (Siemens AG, Munich, Germany) using CuKα radiation in the range 2θ=10-90° and the XRD data was analyzed by using X'Pert package and Fullprof program. The morphology of the obtained materials was examined with a field emission scanning electron microscope (Hitachi FE-SEM model S-4160). FT-IR spectra were recorded on a Tensor 27 (Bruker Corporation, Germany). The thermogravimetric analysis (TGA) has been recorded by STA PT 1600 thermal analysis performed between 25-800°C with the 5°C/min constant rate of heating under air atmosphere in alumina pan. The purity of products was checked by thin layer chromatography (TLC) on glass plates coated with silica gel 60 F254 using n-hexane/ethyl acetate mixture as mobile phase.

Synthesis of $CuBi_2O_4$

In this method, at first 1 mmol $Cu(NO_3)_2$ was dissolved in 25ml of distilled water and stirred for 15min. Then 2 mmol $Bi(NO_3)_2$ was added to the solution and stirred for 15min again. After that, the solution of 25 ml of NaOH (2 M) was added dropwise to receive pH=14. At the end, the solution was transferred to the 100 ml Teflon-lined stainless-steel autoclave for hydrothermal treatment at 180°C for 10 h. When the reaction was completed, it was cooled to room temperature. The obtained $CuBi_2O_4$ was washed with deionized water three times to remove impurity and achieve nurture pH. The prepared powder was washed with distilled water and dried at 110°C for 20 min under normal atmospheric conditions.

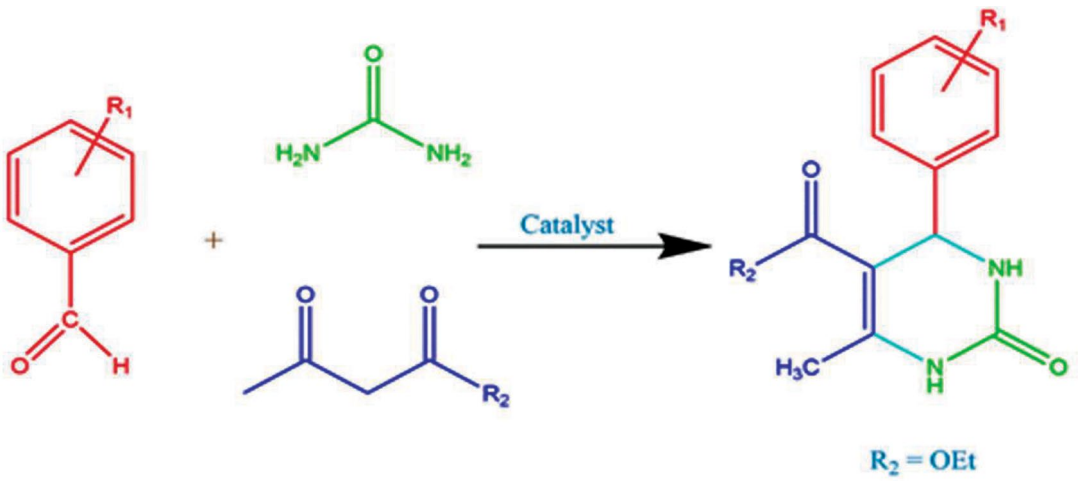

Scheme. 1. Schematic preview for synthesizing DHPMs.

Preparation DHPMs

For synthesizing 3,4 dihydropyrimidin-2-(1H)-ones, a mixture of benzaldehyde (1 mmol), ethyl acetoacetate (1 mmol), urea (1.2 mmol) and different amounts of $CuBi_2O_4$ as catalyst were heated and magnetically stirred in a round-bottom flask under solvent free conditions [28]. The reaction progress was checked by thin layer chromatography (TLC) [6:4 hexane/ ethyl acetate as eluent]. At the end, the solid product was washed with deionized water to separate the unreacted urea for dissolving in water. Then, the precipitation was gathered and dissolved in ethanol to separate the solid catalyst.

RESULT AND DISCUSSION

PXRD analysis

The XRD diffraction pattern of synthesized copper bismuth oxide is shown in Fig. 1. The investigation of XRD data has been done by X'Pert High Score package and Fullprof program [29]. Identification of structure type has been studied by using X'pert package confirms the formation of single phase $CuBi_2O_4$. The results indicate that all the diffraction peaks of $CuBi_2O_4$ can be quite well indexed in tetragonal structure (space group P4/ncc) and the best fit with the least difference is carried out (Fig. 2). Complete adaptability and perfect performance in Rietveld refinement require best amount of initial values and type of space group, which are taken from X'Pert package. The refined lattice parameters are:

$a = b = 8.525$ and $c = 5.822$.

The crystallite size of particles can be calculated by Scherrer's equation:

$$D = (0.94\,\lambda)/(\beta \cos\theta) \quad (1)$$

In this equation, D show particle size, λ is X-ray wavelength (0.154 nm) and β is broadening at half the maximum intensity of the peak. The largest peak is located at 28.008°. The obtained average crystallite size of synthesized $CuBi_2O_4$ nanoparticle is 32nm.

Morphological analysis

For studying the morphology and the sizes of synthesized material FE-SEM was used. Figure 2 shows various magnificent of copper bismuth oxide. This figure shows micro spherical particles that nano cubic forms grow on their surface and create morphology like flower. The size of cuboid which is located on each sphere is between 30-50 nm.

Thermogravimetric analysis (TGA) analysis

Thermogravimetric analysis (TGA) is a technique which determines characteristics of material by gaining weight as a result of increasing temperature. Figure 3 a and b show the TGA and DTA curves of as-prepared $CuBi_2O_4$. The sharp fall at the plot at the beginning up to 100°C belong to losing moisture. After that the sample heated up to 800°C the curve continues with the normal slope which includes no weight loss that emphasizes on nonexistence of organic material and forming pure crystalline tetragonal phase.

Fourier transform infrared spectroscopy (FTIR) analysis

FTIR spectra of as-prepared $CuBi_2O_4$ was observed in Fig. 4. There are two sharp peaks at 3166 cm^{-1} and 3440 cm^{-1} that is attributed to O-H bond stretching. Also, a peak which is located at 1641 cm^{-1} refers to bond bending of H_2O. The peak at 1398 cm^{-1} assigns to stretching vibration of Bi-O bonds [30]. There is a peak at 497 cm^{-1} that is due to stretching vibration of Cu-O bonds [31].

Catalytic studies

Central Composite design and optimal condition in Biginelli reactions

Central composite design (CCD) is broached by Box and Wilson that is one of the most popular methods in response surface methodology (RSM), especially for fitting a second order (quadratic) model [32, 33]. Each factor of this method consists of five levels (-a, -1, 0, 1, a). A CCD is composed of N, the number of experiments, that follow equation:

$$N = 2^k + 2k + C_0 \quad (Eq.\ 2)$$

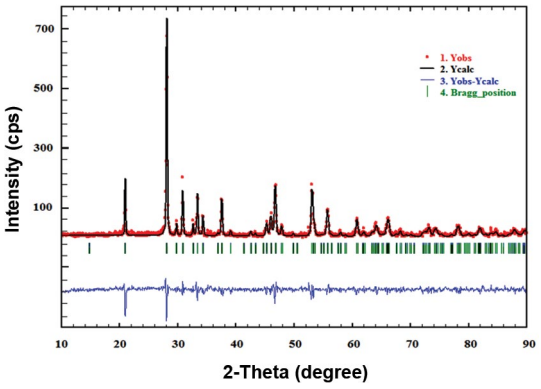

Fig. 1. calculated PXRD pattern for Rietveld profile of synthesized $CuBi_2O_4$.

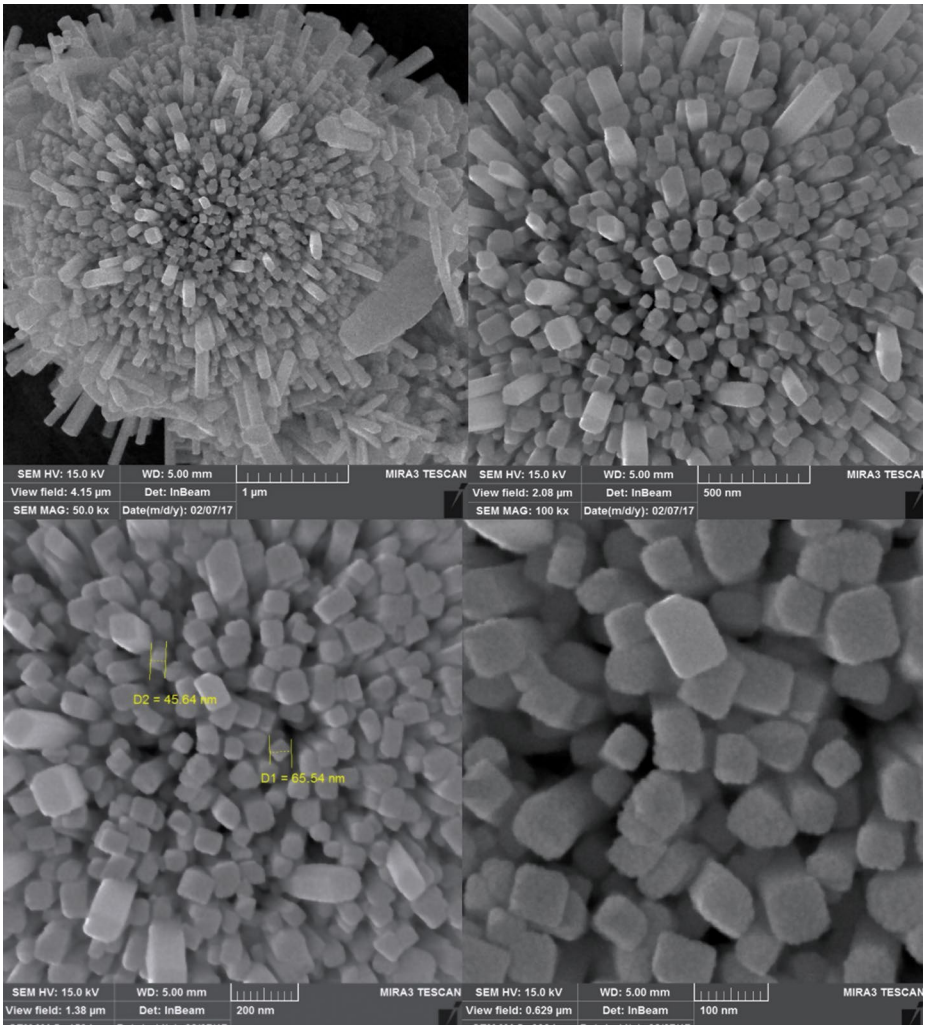

Fig. 2. FESEM images of the hydrothermally synthesized $CuBi_2O_4$ nanomaterials.

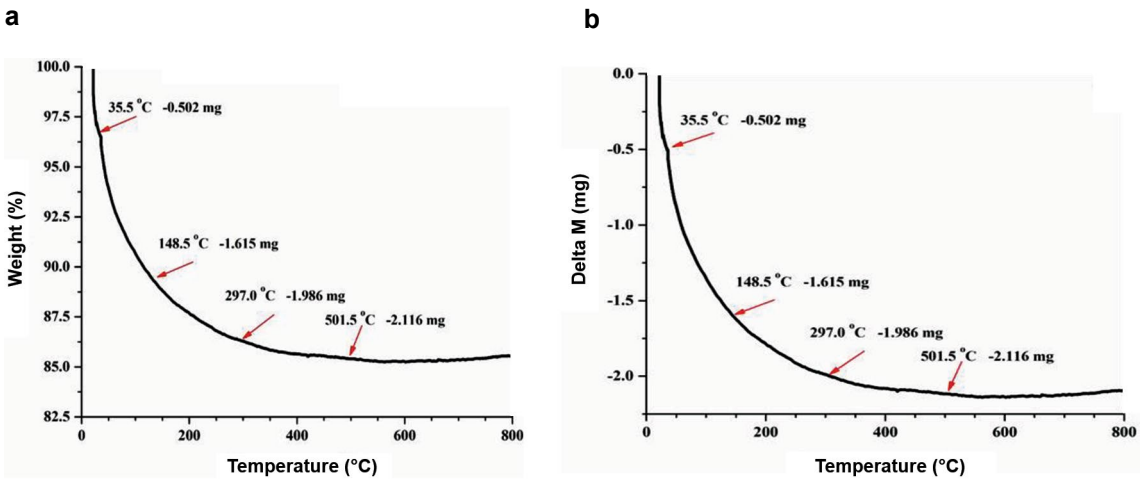

Fig. 3. (a) TGA pattern of $CuBi_2O_4$. (b) DTA pattern of $CuBi_2O_4$.

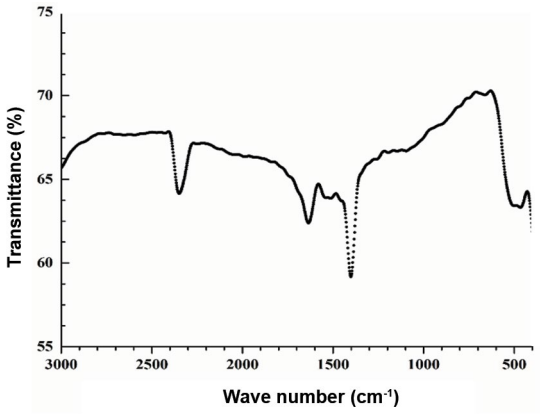

Fig. 4. FTIR spectra of $CuBi_2O_4$.

Where k is the number of factors. 2^k is factorial points, 2k refers to star points and C_0 is the number of central points, respectively [34]. In this research, three effective factors for Biginelli reaction that are the amount of the catalyst (A), temperature (B) and time of the reaction (C) were designed based on CCD as presented in table 1. As it can be seen, this design consists of 5 levels and twenty experiments including six central points and they were performed randomly in three days. Designed condition and the result are reported in table 2.

A collection of mathematical and statistical methods is known as RSM method, which fits N experiments response of the CCD according to the quadratic equation 3:

$$Y = \beta_0 + \sum_{i=1}^{k} \beta_i x_i + \sum_{i=1}^{k} \beta_{ii} {x_i}^2 + \sum_{i<j} \sum \beta_{ij} x_i x_j + \varepsilon \quad \text{(Eq. 3)}$$

In this equation, βs are coefficients which in the first order sentences show main effects and in second order sentences refer to quadratic effects. Also, in the multiplication factors, statements are interaction effects. Y is the response at each experiment, here it is the demonstrated yield of the reaction; x_is are the independent factors. In RSM, by conducting a regression analysis, the coefficients are calculated. In turn, analysis of variance (ANOVA) [35, 36], is used to differ the adequacy of the model.

Analysis of the CCD data which is reported in table 2, by RSM based on equation 3, described the connection between the factors and the yield of the reaction, Y, as shown by equation 4, in which A, B and C are and the same as the coded factors introduced in table 2.

$$Y = 73.06 + 2.01A + 2.96B + 25.71C - 1.25AB + 1AC + 1.5BC - 3.12A^2 - 9.84B^2 - 11.25C^2 \quad \text{(Eq. 4)}$$

The ANOVA of the result model has been presented in table 3. P-value is smaller than 0.1, emphasizing on its significance at high confidence level (90%). As it could be seen from table 3, model had the p-value less than 0.0005, a fact which proves that the model is significant and emphasizes on the significance of the applied quadratic model. The p-value of lack of fit was much more than 0.05, i.e. 0.561, which also confirmed the importance of model. Moreover, the coefficients of determination (the R-square, adjusted–R-square) shows the quality of the fit. In this case, R^2 equaled with 0.9493 that express a high degree of accordance of the response and the independent factors. High value of adjusted regression coefficient (R^2-adj=0.8923) which emphasizes on being as applied model.

To identify the model effect, the three–dimensional (3D) response surfaces plots of the response, based on equation (4), when one factor value was fixed at centre level and two other factors were changed are illustrated in Figures 5a and 5b. The curvature of the plot showed that there was interaction between the factors. It meant that the factors influenced the response interactively and not independently. The purpose of the optimization of factors was to find optimal conditions and define the best condition with the best yield. These conditions were achieved by maximizing the equation (3) when the amount of the catalyst was 0.016 g, at 130°C reaction temperatures, and 57.5 minuet reaction times. In this condition, the yield of experiment is 96%.

Table 1. Factors and levels used in the CCD design

Factors	Symbol	Levels				
		- a	-1	0	1	a
The amount of the catalyst (g)	A	0.002	0.0076	0.016	0.024	0.03
Temperature (˚C)	B	60	78	105	132	150
Time (min)	C	15	32	57	83	100

Table 2. Design matrix and responses for the CCD design

Catalyst amount (g)	Time (min)	Temp (°C)	Yield (%)
day1			
0.0160	58	105	72
0.0243	83	78	10
0.0243	32	132	72
0.0076	32	78	14
0.016	57	105	77
0.0076	83	132	67
day2			
0.0243	32	78	26
0.0160	57	105	63
0.0160	57	105	73
0.0243	83	132	78
0.0076	83	78	19
0.0076	32	132	72
day3			
0.016	57	150	88
0.016	57	105	76
0.016	57	105	77
0.002	57	105	68
0.016	57	60	10
0.016	15	105	38
0.03	57	105	76
0.016	100	105	68

Table 3. Analysis of variance for suggested quadratic model [29]

Source	DF	SS	F	P
Block	2	422.49		
Model	9	12191.95	16.65	0.0003
A	1	55.19	0.68	0.4340
B	1	119.83	1.47	0.2595
C	1	9030.43	111.01	< 0.0001
AB	1	12.50	0.151	0.7053
AC	1	8.00	0.098	0.7618
BC	1	18.00	0.22	0.6506
A2	1	140.12	1.72	0.2258
B2	1	1393.41	17.13	0.0033
C2	1	1822.86	22.41	0.0015
Residual	8	650.76		
Lack-of-fit	5	587.76	5.60	0.5612
Pure error	3	63.00		
Total	19	13265.20		

Recycling and leaching of the catalyst

Reusability of the catalysts is one of the most important factor to make it as an useful economical catalyst. So, checking the recyclability is a significant test. In this section, the reusability efficiency of this product was examined after two times separation and clear that the efficiency doesn't have eye-catching changes. The separation of 3,4-dihydropyrimidin-2(1H)-one from $CuBi_2O_4$ was done by washing with ethanol -three times- and once with chloroform, then centrifuged (EBA 20 Hettich) with 3500 rpm and filtered for separating catalyst. The catalytic reaction was repeated under similar conditions. The yield of the product approximately didn't change a lot -91% and 90% after two times-that is established its recyclability without lacking obvious activity.

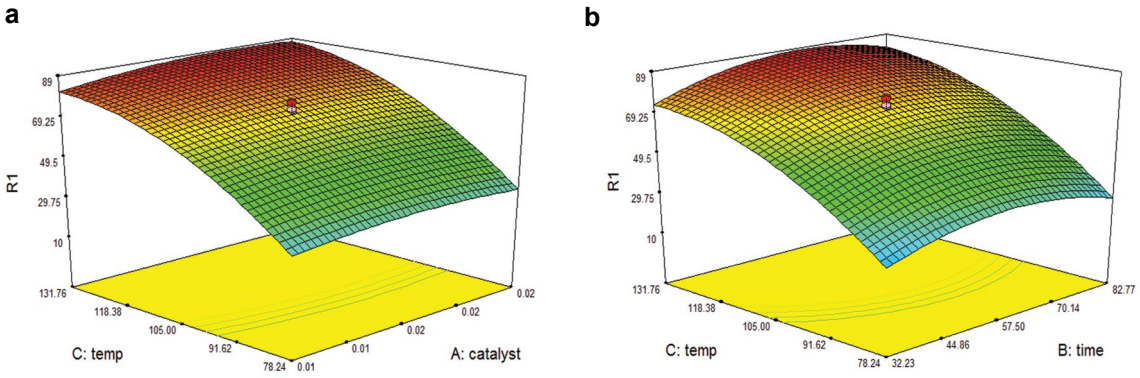

Fig. 5. (a) 3D plot of the response surface of Biginelli reaction (57 min). (b) 3D plot of the response surface of Biginelli reaction (0.016 g).

Table 4. Comparison aspect of the catalytic ability of the CuBi2O4 with other metal oxide

$CuBi_2O_4$	H	1.6×10^{-2} mmol	solvent-free condition, 130°C	96	57 min	This work
RuO_2	H	2.25×10^{-2} mmol	solvent-free condition, 110°C	98	66 min	[30]
$Bi_2Mn_2O_7$	H	2.25×10^{-2} mmol	solvent-free conditions, 104°C	96	66 min	[31]
Fe_3O_4-WCNT	H	0.03 g	Ethanol, reflux, 50°C	98	20 min	[32]
Al_2O_3	H	10mmol	Ethanol at 70°C	31	180 min	[33]
ZnO	H	25 mol%	solvent-free conditions at 90°C	92	50 min	[30]

For obtaining the leaching ability of the catalyst, the reaction has been stopped at half of the reaction time (30min). then the catalyst was separated from the reaction and the progress was continued under same condition. it was explored that no obvious progress was observed on the reaction efficiency (monitored by TLC). This result shows that the continues of the reaction has the direct relationship with existence of catalyst (figure 6).

Comparison catalytic activity

For depicting the efficiency of obtained $CuBi_2O_4$ as catalyst in synthesizing 3,4-dihydropyrimidin-2(1H)-ones, it is compared with other reported metal oxides. which is shown in table 4. As it is seen, the yield of product, by considering time, temperature and amount of catalyst, for $CuBi_2O_4$ nanoparticle in comparison with other reported catalysts is undeniable.

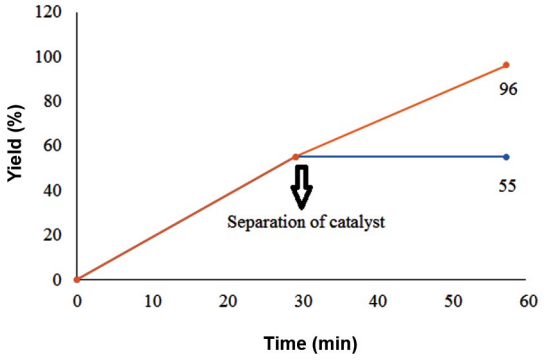

Fig. 6. Hot filteration test of the catalyst under free solvent condition.

CONCLUSION

This research demonstrates synthesis of single phase $CuBi_2O_4$ by one-step hydrothermal method successfully. The experimental conditions caused to create the morphology like flower of cupper bismuth oxide, such as sphere microparticles with numerous cubic particle on its surface. In addition, catalytic property of obtained material was investigated and the results indicated perfect performance and high yield of this metal oxide. Also, $CuBi_2O_4$ has low toxic property, an ecofriendly and a chemically stable catalyst, high reusability performance, also it has easier separation and work up.

ACKNOWLEDGMENT

We thank Semnan University for supporting this study.

CONFLICT OF INTEREST

The authors declare that there is no conflict of interests regarding the publication of this manuscript.

REFERENCES

1. G.D. Rao, B. Anjaneyulu, M. Kaushik, G. Prasad. Int. J. Eng. Sci. Paradigms and Researches, 2319 (2015)
2. G.J. Grover, S. Dzwonczyk, D.M. McMullen, D.E. Normandin, C.S. Parham, P.G. Sleph, S. Moreland, J. Cardiovasc. Pharmacol, 26, 289 (1995).
3. C.O. Kappe, Acc. Chem. Res., 33, 879 (2000).
4. C.O. Kappe, Eur. J. Med. Chem., 35, 1043 (2000).
5. P. Biginelli, Eur. J. Inorg. Chem., 24, 1317 (1891).
6. D. Girija, H.S. Bhojya Naik, B. Vinay Kumar, C.N. Sudhamani, K.N. Harish, Arab. J. Chem., (2014), (in press).
7. A.J. Sabbaghian, P. Nasehi, Int. J. Heterocycl. Chem. 3, 29 (2013).
8. J. Safari, S. Gandomi-Ravandi, J. Mol. Struct., 1074, 71 (2014).
9. J. Safari, S. Gandomi-Ravandi, JJ. Mol. Catal. A: Chem., 373, 72 (2013).
10. O. Fedorova, M. Valova, Y. Titova, I. Ovchinnikova, A. Grishakov, M. Uimin, A. Mysik, A. Ermakov, G. Rusinov, V. Charushin, Kinet. Catal., 52 (2011).
11. F. Soleimani, M. Behzad, M. Salehi, J. Nanostruct., 5, 351 (2015).
12. J. Safari, Z. Zarnegar, RSC. Adv., 3, 17962 (2013).
13. S. Khademinia, M. Behzad, A. Alemi, M. Dolatyari, S.M. Sajjadi, RSC. Adv., 5, 71109 (2015).
14. J. Boivin, J. Tréhoux, D. Thomas, Bulletin de la Societe Francaise Mineralogie ET de Crisallographie, 99, 193 (1976).
15. T. Arai, M. Yanagida, Y. Konishi, Y. Iwasaki, H. Sugihara, K. Sayama, J. Phys. Chem. A, 111, 7574 (2007).
16. T. Arai, Y. Konishi, Y. Iwasaki, H. Sugihara, K. Sayama, J. Comb. Chem., 9, 574 (2007).
17. N.T. Hahn, V.C. Holmberg, B.A. Korgel, C.B. Mullins, J. Phys. Chem. C, 116, 6459 (2012).
18. J. Zhang, Y. Jiang, J. Mater. Sci. - Mater. Electron., 26, 4308 (2015).
19. F.-J. Zhang, F.-Z. Xie, J. Liu, W. Zhao, K. Zhang, Ultrasonics sonochemistry, 20, 209 (2013).
20. M. Bhat, B. Chakravarthy, P. Ramakrishnan, A. Levasseur, K. Rao, Bulletin of Materials Science, 23, 461 (2000).
21. X. Chen, Y. Dai, J. Guo, Mater. Lett., 161, 251 (2015).
22. S. Sobanska, J.-P. Wignacourt, P. Conflant, M. Drache, I. Bulimestru, A. Gulea, Eur. J. Solid State Inorg. Chem., 33, 701 (1996).
23. S. Jones, J. Akridge, Singapore: world Scientific, 2, O9 (1995).
24. E. Abdelkader, L. Nadjia, B. Ahmed, Journal of King Saud University-Science, 27, 76 (2015).
25. M. Chen, Q. Yang, L. Li, M. Liu, P. Xiao, M. Zhang, Mater. Lett., 171, 255 (2016).
26. D. Cao, N. Nasori, Z. Wang, Y. Mi, L. Wen, Y. Yang, S. Qu, Z. Wang, Y. Lei, J. Mater. Chem. A, 4, 8995 (2016).
27. J. Garcia-Munoz, J. Rodriguez-Carvajal, F. Sapina, M. Sanchis, R. Ibanez, D. Beltran-Porter, J. Phys.: Condens. Matter, 2, 2205 (1990).
28. H. Valizadeh, A. Shockravi, Heteroat. Chem, 20, 284 (2009).
29. J. Rodrigueg-Carvajal, Laboratorie Leon, Brillounin, Gifsuryvette, France, (2009).
30. F. He, Z. He, J. Xie, Y. Li, Am. J. Anal. Chem., 5, 1142 (2014).
31. A.A. Radhakrishnan, B.B. Beena, Indian J. Adv. Chem. Sci., 2, 158 (2014).
32. H.J. Kelley, Math. Sci. Eng., 5, 205 (1962).
33. R. Myers, D. Montgomery, C. Anderson-Cook, Response Surface Methodology. 3rd, New York, NY, USA: John Wiley and Sons, (2009).
34. P. GE, KB Wilson, J Royal Stat Soc, Senes B, 13, 1 (1951).
35. R. Myer, D.C. Montgomery, John Wiley and Sons, New York, 343 (2002).
36. R.H. Myers, D.C. Montgomery, G.G. Vining, C.M. Borror, S.M. Kowalski, J. Qual. Technol., 36, 53 (2004).